Proceedings of International Conference on Heat Exchanger Fouling and Cleaning - 2013 (Peer-reviewed)
June 09 - 14, 2013, Budapest, Hungary
Editors: M.R. Malayeri, H. Müller-Steinhagen and A.P. Watkinson
Published online
www.heatexchanger-fouling.com

DEPOSITION FROM A SOUR HEAVY OIL UNDER INCIPIENT COKING CONDITIONS: EFFECTS OF SURFACE MATERIAL AND TEMPERATURE

W. Wang* and A. P. Watkinson

Department of Chemical and Biological Engineering, The University of British Columbia
2360 East Mall, Vancouver, BC, Canada V6T 1Z3
wwang@chbe.ubc.ca

ABSTRACT

Fouling in vacuum tower furnaces has been a great challenge in refineries. At the elevated temperatures of these units, coke deposition is common. For sour oils, iron sulphide also accumulates in the carbonaceous deposits, arising from iron dissolved in the feed or from corrosion of metal surfaces. In this work, the combined fouling mechanism is investigated using an atmospheric tower bottom stream which contains 4.1 % wt. sulphur, and 710 wppm dissolved iron. Isothermal deposition experiments running for 6-24 hours have been carried out on a rotating cylinder in a 600 ml batch reactor, at bulk temperatures of 380-410°C, and cylinder rotation speeds of 300rpm. A ring of either carbon steel or alloy is mounted in the cylinder to serve as a corroding or non-corroding surface, respectively. After each experiment, the thickness and weight of deposit on the metal ring are determined. The compositions of deposit are characterized. The rates of deposit formation on the ring and the deposit composition are reported as functions of temperature for a number of metal surfaces. Radial profiles of deposit composition are presented. The probable fouling mechanisms are discussed, based on the present results.

INTRODUCTION

Fouling of furnaces negatively affects profitability of refinery operations (Lemke and Stephenson, 1998), and leads to increased CO_2 emissions. Vacuum tower furnaces are widely used to heat atmospheric tower bottoms (ATB) for vacuum distillation. Typically, furnace outlet temperatures are in the range 390°C to 450°C (Gary and Handwerk, 2001). ATB is a highly viscous and polar heavy oil fraction, of high molecular weight and significant concentrations of asphaltenes, which has a strong tendency to convert to coke under furnace operating conditions (Lemke, 1999). Several mechanisms have been proposed to describe coking reactions (Albright and Marek, 1988; Dickakian and Seay, 1988).

Wiehe proposed a phase-separation kinetic model for coke formation (Wiehe, 1993; Wiehe, 2008). According to this model, as side-chains are removed during heating, the resultant asphaltene cores eventually reach a solubility limit in the surrounding fluid. As the conversion of residue continues, asphaltene cores form a new phase, in which donor hydrogen is insufficient, and the asphaltene radicals recombine in this phase to form coke.

Sulphidic corrosion is widely observed in oil processing especially above temperatures of 260°C (Zetlmeisl, 1996). In sour oils, concentrated sulphur compounds, which will react with iron both on the tube surface and in the oil, to generate iron sulphide. Thus iron sulphide has been a key component of foulants in heat exchangers (Ebert and Panchal, 1995) and furnaces (Parker and McFarlane, 1999; Wang and Watkinson, 2011). Taylor (1976) observed significantly higher deposit formation rate in deoxygenated jet fuel with added sulphides, di-sulphides, poly-sulphides and thiol while thiophene did not promote the deposit formation. Three mechanisms for corrosion of iron chromium alloys in sulphur vapour were proposed (Mrowec et al., 1969) according to the level of chrome in the alloy. They also found the sulphidation of all the alloys follows a parabolic rate law. Pareek et al. (1994) studied sulphidation corrosion of 4130 steel in vapour phase CH3SH and found two rate determining steps of surface reaction for both high temperature (370-550°C) and low temperature (250-370°C), respectively.

The objectives of this research were to explore the rates of iron sulphide and carbonaceous matter deposition as a function of temperature, and wall shear stress on both non-corroding and corroding surfaces. Focusing on deposit composition can elucidate the relative roles of iron sulphide and coke deposition at temperatures where incipient coking occurred in the bulk fluid. The native iron content of the oil chosen for this work is sufficient to lead to iron sulphide deposition in the absence of corrosion. Radial elemental distribution in the deposit was measured to aid in establishing mechanisms of the deposition process involved on corroding and non-corroding surfaces.

EXPERIMENTAL

Isothermal fouling experiments were performed in a 600 ml Parr instrument Model 4563 stirred rotating cylinder batch reactor (Figure 1). A glass liner prevents the direct contact of hot oil with the interior metal wall of the reactor. The reactor is shown schematically in Figure 1. A rotary cylinder consisting of annular rings of different metals with outside diameter of 3.81cm and height of 1cm was fixed to

two flanges of the same diameter made from MACOR, a type of machinable ceramic which has stable physical and chemical properties at high temperatures. A magnetic drive with a controller was used for rotating the cylinder. The rotation speeds were determined with a REED AT-6 tachometer. Two thermocouples were connected with Omega CN76000 controllers, to adjust the heater temperature, T_h, as well as bulk oil temperature, T_b, with a PID mode, respectively, to achieve precise control and a repeatable liquid heat-up procedure. An Omega OMB-DAQ-54 data acquisition module was used to record heater and bulk temperature, as well as the pressure during experiments.

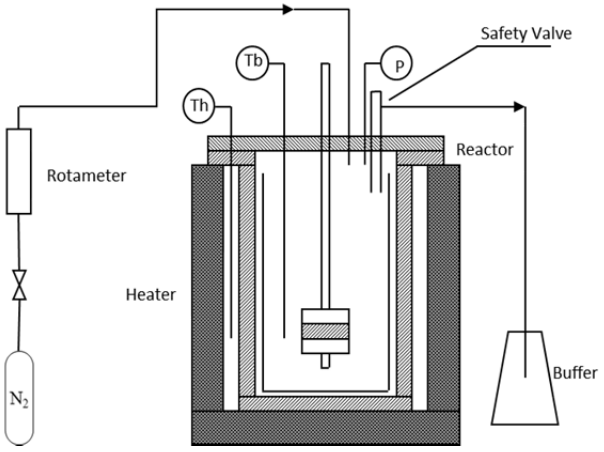

Fig. 1 Structure of rotating cylinder batch reactor

An atmospheric tower bottom (ATB) oil sample provided by Syncrude Canada Ltd. has been used. The physical and chemical properties of the ATB oil are listed in Table 1. The elemental analysis of metallic constituents was determined by Inductively Coupled Plasma (ICP).

Five types of metal surfaces, which are widely used in different parts of vacuum tower furnace, were investigated, including type 1018 low carbon steel (CS), type 317 stainless steel (SS317), ASTM A387 grade 9 chrome steel (9-chrome), Incoloy alloy 825 (Incoloy 825), and chrome plated carbon steel (0.127mm thickness of chromium layer) on the surface (Cr-CS). Chemical composition ranges of the metals are shown in Table 2 (Perry and Green, 2007).

Before experiments, the rings were polished with 4 types of emery paper of 360-1500 grit in order to obtain a constant initial surface roughness, which was measured by a Mitutoyo SJ-210 surface roughness tester. Using this procedure, the roughness of the metal surface was in the range of 0.31-0.36μm. The rings were rinsed with toluene in order to remove all liquid constituents including asphaltenes from the deposit, and then dried in air. Dissolved oxygen is claimed an essential factor to induce fouling, especially on clean steel surfaces (Jones and Balster 1995). Therefore, dissolved air was removed with nitrogen before elevating the temperature to prevent rapid coking. In the heating process, temperature was elevated from 110°C to the required temperature within 1 hour. Tests showed that no significant thickness and mass change occurred during the heating process. It is reported that the maximum temperature for naphthenic acids to be stable is 370°C. Above this temperature thermal decomposition occurs (Turnbull et al., 1998). Therefore we assume that naphthenic acids decompose rapidly in the fast heating process.

Table 1. Properties of ATB

Property	Value
25°C Density, g/cm^3	1.0215
Ash (wt. %)	1.45
MCR	14.98
Mass, wt.%	
C	83.1
H	9.65
S	4.088
N	0.45
Partial Elemental Analysis, wppm	
Si	775
Fe	744
Al	658
V	142
Ca + Mg	186
K	95
Ti	80
Ni	73

Table 2. Partial Chemical Composition Ranges of Metals (% wt.)

Metal	Fe	C	Cr	Mo	Ni
CS	98.81 - 99.25	0.15 - 0.2			
Cr-CS			100 (surface)		
SS317	57.8 - 65.8	0.08 max	18 - 20	3 - 4	11 - 15
Incoloy 825	21.0 - 36.1	0.05 max	19.5 - 23.5	2.5 - 3.5	38 - 46
9- chrome	87.1 - 89.6	0.15 max	8 - 10	0.9 - 1.1	

*Sulphur content is 0.05 % wt. for CS, 0 for Cr-Cs and 0.03 % wt. for the other 3 alloys.

In the present work, the bulk temperature range investigated was 380-410°C. The experiment duration was set to 24 hours after the heat-up procedures when the bulk temperature achieved the desired value, and the rotation speed of the cylinder was fixed at 300rpm. The wall shear

stress can be calculated as (Silverman, 1984; Efird et al., 1993):

$$\tau_w = 0.079Re^{-0.3}\rho u_{cyl}^2 \quad (1)$$

In which,

$$\mathrm{Re} = \frac{d_{cyl}u_{cyl}\rho}{\mu} \quad (2)$$

$$u_{cyl} = \omega r_{cyl} = \frac{\pi d_{cyl}F}{60} \quad (3)$$

The corresponding calculated wall shear stress, τ_w, is 2.0-2.2Pa and Reynolds number is 3000-3900.

At the end of experiments, the temperature of the reactor was decreased rapidly to around 90°C by cooling with a fan blower. Rings were taken out and rinsed with toluene to remove the attached liquid oil on the deposit, and dried for 24 hours in air. Since using a micrometer may probably squeeze the deposit or even destroy it during measurement, the thickness of deposit was calculated from a photographic method. Images were taken via a microscope equipped with a 4X lens for both a 0.1mm gap of a micrometer, as well as the cross-section of ring with deposit. Then the thickness of deposit was calculated using the relative lengths of the gap and deposit. For each ring, 8 locations were measured to allow calculation of an average thickness and standard deviation. The weight change of rings before and after experiments was measured using an analytical balance with an accuracy of 0.1mg, to give the rate of mass build-up. The deposit was characterized with Thermogravimetric Analysis (TGA), using a "proximate" analysis for fuels, which yields a measure of volatiles, fixed carbon and ash. In the present context, volatiles represent the weight percentage of the deposit which evaporates at temperatures up to 900°C in a nitrogen atmosphere. This is mainly the oil fraction with boiling point from low to high. Fixed carbon represents the fraction which does not evaporate at 900°C but is able to be burned in air. Fixed carbon can be considered as coke. Ash is the remaining fraction after the deposit is burned in air at 900°C, and can arise in the deposit from either metallic contaminants in the oil, or from corrosion of the metal surface. In this paper, we consider the deposit as comprising two fractions: % ash and % carbonaceous matter, where the latter is the sum of the % volatiles and the % fixed carbon from the TGA measurement.

For the purpose of investigating the composition of deposits at different distances from the surface, radial profiles of deposit have been examined with SEM-EDX. Before the SEM-EDX tests, the ring with the deposit attached was mounted in epoxy for protection. The cross section was polished with 200-1000 grit emery paper, then with 6μm and 1μm diamond paper consequently to achieve a sufficiently smooth, flat surface for EDX measurements. Three locations of each ring were selected for analysis.

RESULTS AND DISCUSSION

Results are first discussed below in terms of deposit thickness, mass, and bulk composition on the various surfaces after 24 hours, as functions of temperature. Subsequent examination of radial profiles variation over the 20μm from the metal surface allows a focus on the initial steps in deposit build-up.

a) Effect of Bulk Oil Temperature on the Thickness of Deposit

Figure 2 shows microscopic images of deposits on SS317 (Upper) and on CS (Lower). The thickness of deposit is roughly 240μm for the SS317, and 54μm for the CS. Eight images are taken at different locations around the rings for calculation of the average thickness and standard deviation.

Figure 2 also shows two typical morphologies for the deposit accumulated on metal surfaces. For the SS317 surface, the deposit adheres tightly to the surface. For the CS at the lowest temperature tested, a gap appears between a loose, poorly attached layer which surrounds the surface. This layer can easily be dislodged from the surface and drop into the fluid. A possible reason for this is seen in section b) below.

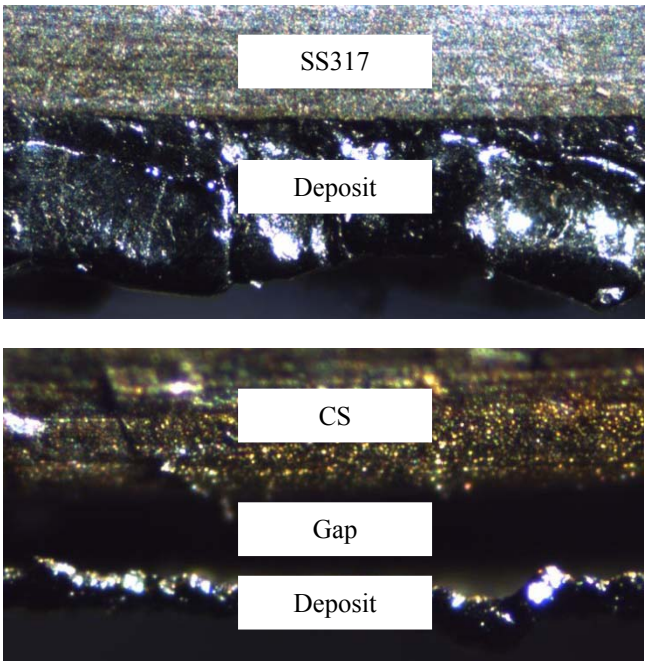

Fig. 2 Microscopic images of deposit for two experiments of 24h at 300rpm (Upper: SS317 at 400°C Lower: CS at 380°C)

Figure 3 shows the effect of bulk oil temperature on the deposit thickness at fixed experiment duration and rotation speed. Thickness increases with bulk oil temperature for all five surfaces. Deposit thicknesses at bulk temperature of 380°C on all surfaces are quite close to each other, and

below 75μm. At 390-400°C, the five surfaces can be divided into two groups based on deposit thickness. The deposit on CS and 9-chrome surfaces is significantly thicker (~ 300-400μm) than the other three surfaces (75-200μm). Deposit on CS and Cr-CS surface increased sharply at 410°C, while the amount of deposit for the other three surfaces did not change markedly compared to the values of 400°C. Chromium has been proven effective as a dehydrogenation catalyst (Lugo and Lunsford, 1985; Reyniers and Froment, 1995); hence it may increase coke formation at 410°C for the Cr-CS.

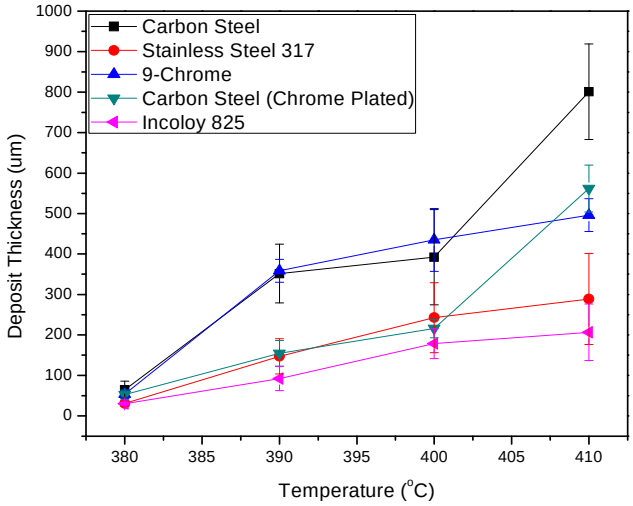

Fig. 3 Effect of bulk oil temperature on thickness of deposit on rings with different metal surface for 24-hour experiments at 300rpm.

b) Effect of Bulk Oil Temperature on the Overall Composition and Mass of Deposits

Figure 4 shows the effects of bulk oil temperature on weight percentage of carbonaceous matter in deposits. The remainder is ash. For the Cr-CS ring, deposits were over 90% carbonaceous matters at all temperatures. For the CS and 9-chrome, the percentage carbonaceous matter increased sharply with temperature, from about 20-30% at 380°C, to 90% at 410°C. For SS317 and Incoloy 825, deposits were 75-90% carbonaceous matter at low temperature and 95% at 410°C. At 410°C, deposits are 91-99 % wt. carbonaceous matter for all metals tested. This reflects the dominance of the coking reactions in forming deposits at high temperatures.

As mentioned in section a), two different morphologies of deposit have been observed. Actually the loose layer only occurred on CS and 9-chrome surface at bulk oil temperature of 380°C, where the weight percentage of ash in the deposit is higher than 70%. For higher temperatures of these two surface materials and at all temperature of the other three, a tightly adherent layer was obtained. This may be due to the composition of deposit. It is assumed that if there is a significant weight percentage of ash, the deposit layer is not so solid and is easily dislodged from the metal. However, if most of the deposit is carbonaceous, it attaches rather tightly to all metals.

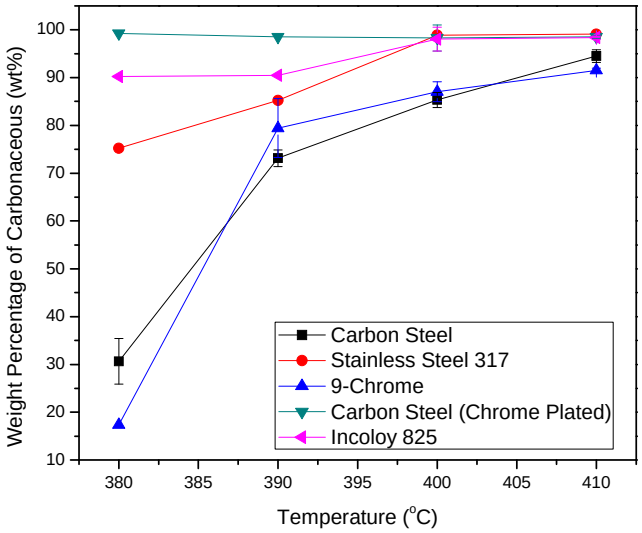

Fig. 4 Effect of bulk oil temperature on weight percentage of carbonaceous matter of deposit on rings with different metal surface for 24-hour experiments at 300rpm

Figure 5 shows the effect of bulk oil temperature on the total mass of deposit at fixed experiment duration and rotation speed. The change of mass was very similar with change of thickness in Figure 3, which indicates both mass and thickness measurement are reliable methods for investigating the accumulation of deposit on metal surfaces.

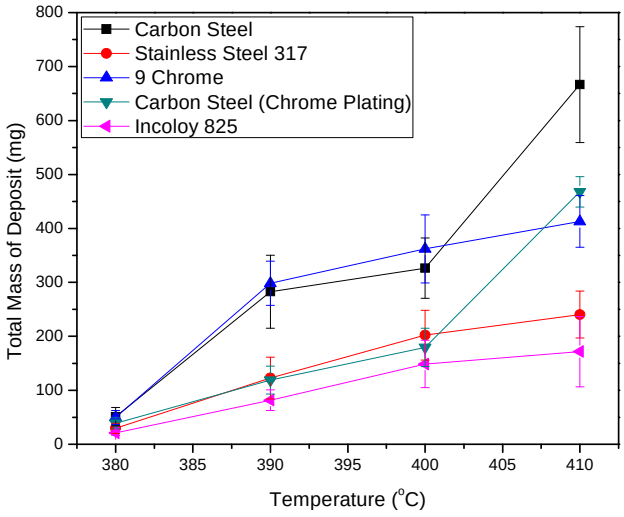

Fig. 5 Effect of bulk oil temperature on total mass of deposit on rings with different metal surface for 24-hour experiments at 300rpm

c) Effect of Bulk Oil Temperature on the Mass of Ash and Carbonaceous Deposits.

Figure 6 indicates the effect of bulk oil temperature on the mass of ash in the deposits at fixed experiment duration and rotation speed. For chrome-plated CS, the mass of ash in the deposit after 24 hours increased uniformly from 0.3mg to 6.9mg as temperature was raised; however, for the other four surface materials, there was a maximum mass of ash at bulk oil temperature of 390°C. Above this temperature, coke formation dominated, and appeared to reduce ash accumulations on these surfaces. For the SS317, and Incoloy 825, the ash content was slightly higher than the Cr-CS, and generally below 10 mg. For CS and 9-chrome, the mass of ash on each metal was very similar, and considerably higher (range 30-60 mg), except for a slightly larger difference at 390°C.

There are two potential sources of ash in the deposits: corrosion products of the metal surface and inorganic compounds in the oil (Table 1). Since the mass of ash for CS and 9-chrome is around 5-10 times of that of the other three metal surfaces, most of the ash for CS and 9-chrome presumably comes from corrosion products.

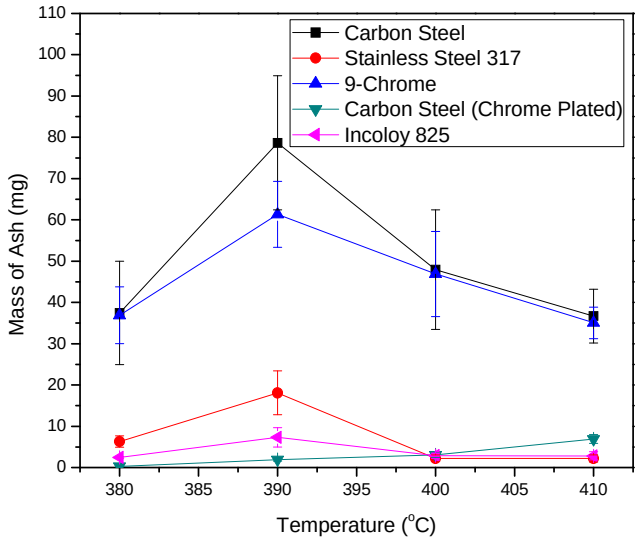

Fig. 6 Effect of bulk oil temperature on mass of ash in deposit on rings with different metal surface for 24-hour experiments at 300rpm

Figure 7 shows the effect of bulk oil temperature on the mass of carbonaceous matter in deposits at fixed experiment duration and rotation speed. The trend was similar to the change of deposit thickness with temperature shown in Figure 3. It should be noted that at 380°C, both deposit thickness and mass of carbonaceous deposit for all five surfaces were similar to each other. At 390°C and 400°C, CS and 9-chrome had remarkably higher value for both thickness and mass of carbonaceous deposit than on the other three metal surfaces. Considering the mass of ash in Figure 6, the inorganic metal compounds apparently play a key role in this stage in promoting the accumulation of carbonaceous deposit.

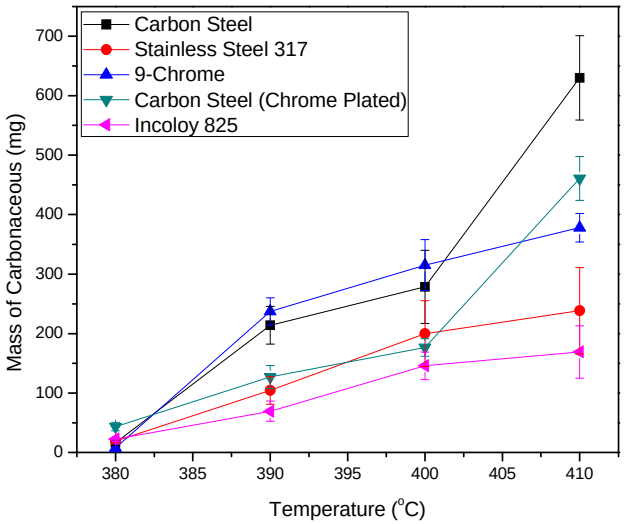

Fig. 7 Effect of bulk oil temperature on mass of carbonaceous matter in deposit on rings with different metal surface for 24-hour experiments at 300rpm

d) Radial Deposit Composition Profiles in the Wall Region

Figure 8 is an SEM image of the cross-section of a Cr-CS ring with deposit, mounted in epoxy and polished. The thickness of deposit is about 60μm. The layer of chrome plating is about 110μm thick.

Figure 9 shows the cross-section of a carbon steel ring with deposit, taken at higher magnification. Due to the large thickness and magnification the deposit thickness cannot be determined in the image. Fragmentation is observed at the border of CS.

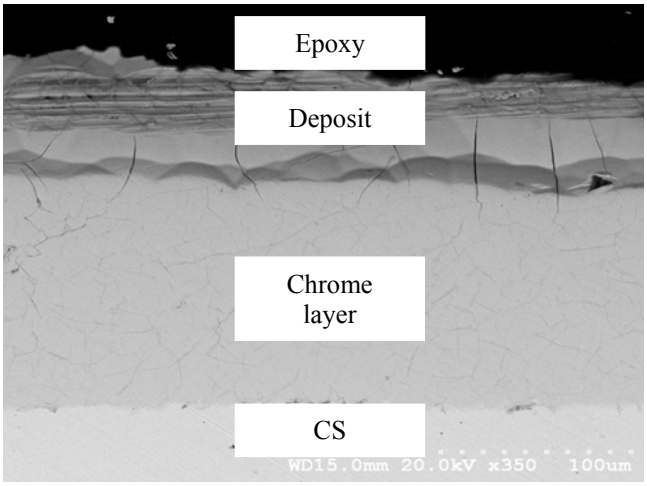

Fig. 8 SEM image of deposit on Cr-CS surface after a 24-hour experiment at 390°C and 300rpm (WD15.0mm, 20.0kV, ×350)

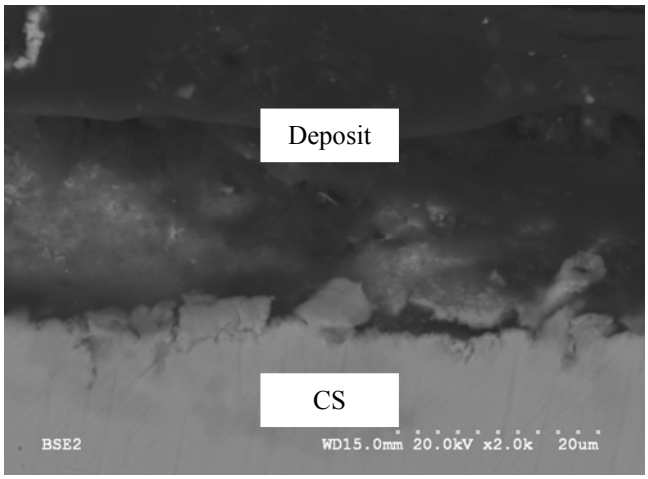

Fig. 9 SEM image of deposit on CS surface after a 24-hour experiment at 390°C and 300rpm (WD15.0mm, 20.0kV, ×2000)

Figures 10-12 are radial profiles of iron, carbon and sulphur, respectively, from the surfaces to a 20µm thick outer layer at fixed bulk oil temperature, rotation speed and experiment duration. The zero value on the X-axis refers to a position just inside of the metal. Four additional reference lines with different distances from the metal surface were taken to measure the weight percentage of key elements, including iron, sulphur, carbon, chromium, nickel, etc.

Figure 10 shows that, with the exception of the Cr-CS surface, weight percentage of iron in deposits decreased rapidly in a very small distance (~5µm) from the surface. For CS and 9-chrome, the iron concentration values kept decreasing gradually with distance after 5µm, while for the other three surfaces, a relative constant value was achieved after 5-10µm.

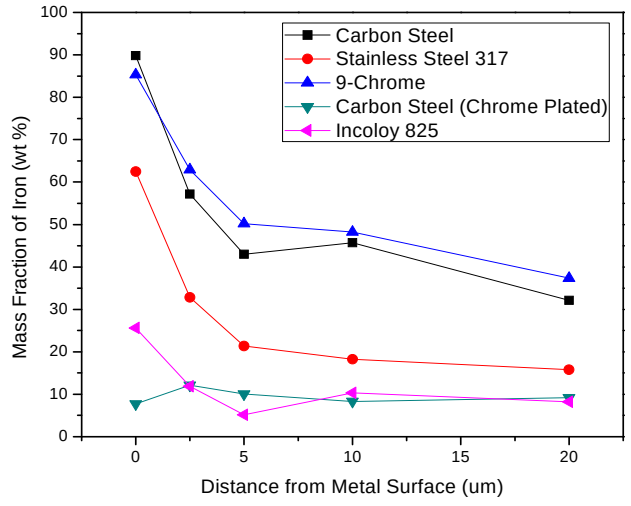

Fig. 10 Radial distribution of iron in deposit after a 24-hour experiment at 390°C and 300rpm

Figure 11 indicates that weight percentage of carbon increased strongly with distance. For Cr-CS and Incoloy 825, the surfaces were covered with almost pure (>85%) carbonaceous coke after a short distance of a few microns. For the other three surfaces, there was a transition zone of at least 20µm in which carbonaceous deposit mixes with inorganic ash.

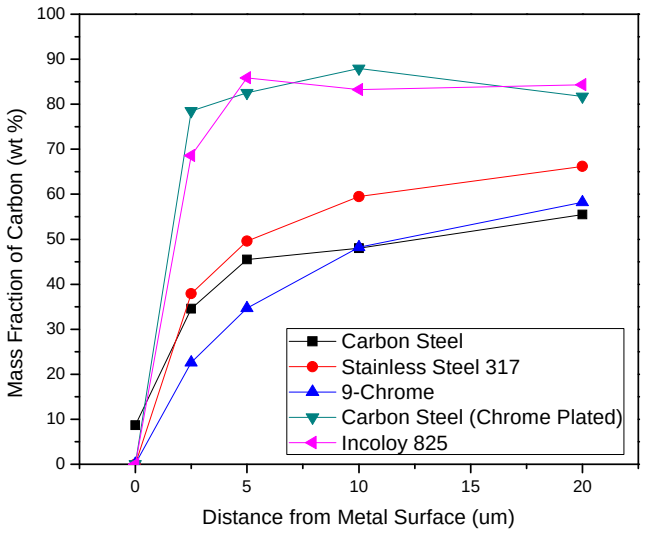

Fig. 11 Radial distribution of carbon in deposit after a 24-hour experiment at 390°C and 300rpm

In Figure 12, the sulphur weight percentage was highest (5-8 % wt.) in the zone very close (~2.5µm) to the metal, for Incoloy 825, SS317 and Cr-CS. It then dropped sharply to about 3 % wt. For CS and 9-chrome, beyond a few microns the weight percentage of sulphur gradually decreased with distance in a longer scale.

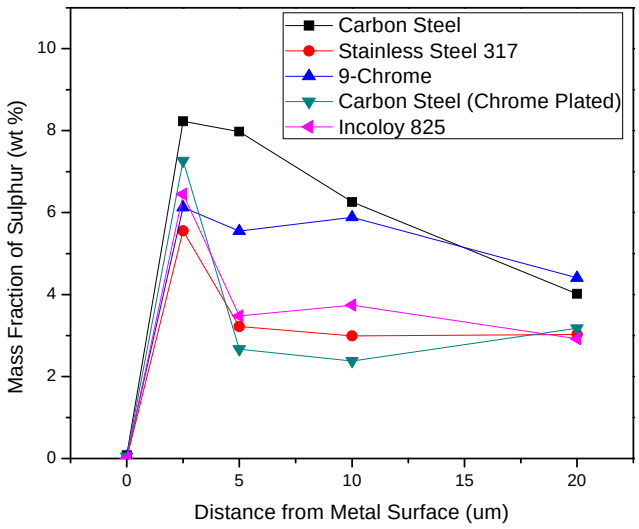

Fig. 12 Radial distribution of carbon in deposit after a 24-hour experiment at 390°C and 300rpm

The atom ratio of Fe/S can be calculated from Figure 10 and Figure 12. Beyond 5µm distance, for Incoloy 825 and Cr-CS, the Fe/S atomic ratio was about 1-2, while for CS, 9-chrome and SS317, the Fe/S ratio was around 3-6. In feed oil, this ratio is 0.01, which suggests that most of the iron in the deposit is from corrosion of the metal surfaces.

Further information may be gained from examining ratios of key metals in the system to indicate whether iron and other metals transfer from the metal surface into the deposit and fluid. Nickel and vanadium mainly accumulate in similar oil components (such as porphyrins). The atomic ratios of nickel and vanadium to iron were calculated for feed oil, metal, and deposit, and are shown in Table 3.

Table 3. Atomic Ratio of Nickel and Vanadium to Iron in ATB, Metal and Deposit (SS317 and Cr-CS)

	Ni/Fe	V/Fe
SS317		
ATB	0.093	0.209
Metal surface	0.191	0
Deposit	0.189-0.191	0.007-0.009
Cr-CS		
ATB	0.093	0.209
Metal surface	0	0
Deposit	0.101	0.178

Romeo et al (1971) found nickel in the outer layer of the scale formed when nickel-chrome alloys are sulphided at high temperature. For the SS317, the Ni/Fe in the deposit is similar to that in the metal (Ni/Fe ≈ 0.19), and much above that in the ATB. Hence the deposit inorganic content appears to originate from the metal. The V/Fe ratio in the ATB (V/Fe ≈ 0.21) is much larger than that in the deposit (V/Fe ≈ 0.01), which supports the argument that the deposit inorganic material is from the metal. For the Cr-CS, both the Ni/Fe and V/Fe ratios in the deposits are similar to the respective values in the ATB. Hence the deposits appear to originate in the ATB and corrosion of the metal does not play a significant role.

Figure 13 shows the influence of chromium contents in metals on the weight percentage of iron at locations of different distance from surfaces. For Cr-CS, the chrome plating is assumed thick enough that the surface behaves as 100 % chromium. Sudden changes were seen when weight percentages of chromium in metals were 15-20 % wt... When chromium content was 20 % wt. or higher, the Fe contents in deposit was decreased to around 1/5 of the value when chromium content was lower than 15 % wt... The effect of chromium on corrosion performance has been widely studied in other systems. Mrowec et al. (1969) proposed 3 mechanism of formation of scales corresponding to 3 chromium content for low (up to 2 % at.), intermediate (2-40 % at.) and high (above 40 at. %) in sulphur vapour at 700-1000°C. Corrosion test in 1 N HCL by Naka et al. (1979) indicated addition of up to 20% at. of chromium to boron-bearing alloys doesn't affect the corrosion resistance; while the addition of 30 % at. or more chromium significantly decreases the corrosion rate. Delabrouille et al. (2005) believed that in 360°C water, continuous and compact layer of chromium oxide formed for alloys which contain more than 10% chromium. This layer would cover the metal surface.

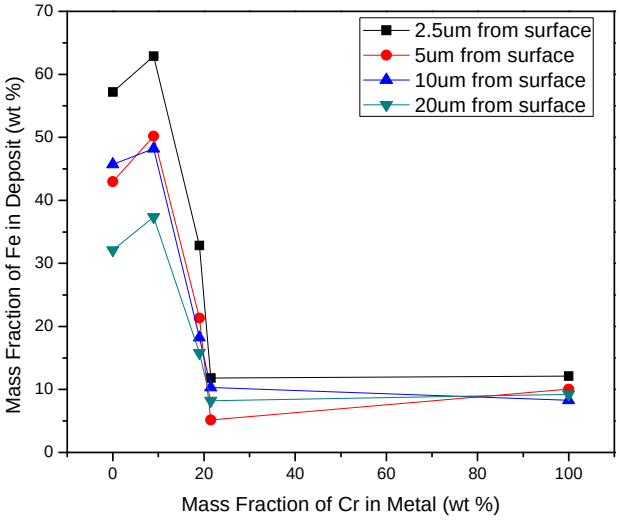

Fig. 13 Effect of weight percentage of Cr in the metal rings on the weight percentage of Fe in deposit at different distances from the metal surface after a 24-hour experiment at 390°C and 300rpm

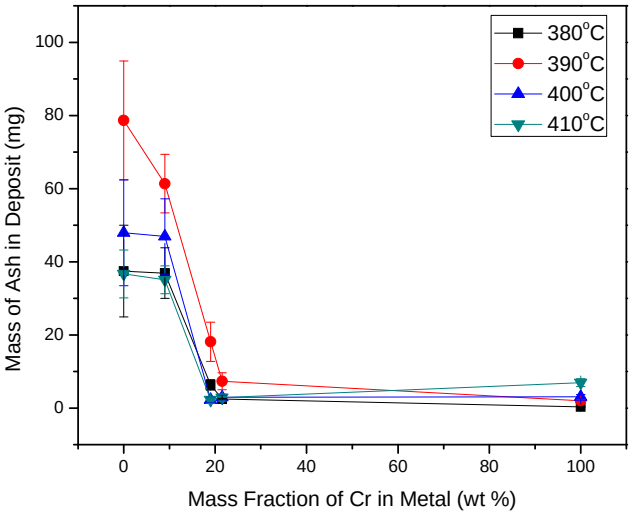

Fig. 14 Effect of weight percentage of Cr in the metal rings on the mass of ash in deposit at different temperatures after a 24-hour experiment at 300rpm

Figure 14 illustrates the influence of chromium contents in metals on the mass of ash in deposit at different temperatures, which reveals the corrosion resistant performance of different alloys. In Figure 14, the mass of ash in deposit was significantly affected by temperature,

and was much higher when the mass fraction Cr in the metal was less than about 15-20 % wt... However, for the alloys containing more than 15-20 % wt. chromium, the mass of ash was evidently lower than that on the other low chromium content alloys, and was not very dependent on bulk temperatures. This also proves that 15-20 % wt. of Cr content is a boundary for metals which perform different in high temperature sulphidic corrosion.

CONCLUSIONS

1. Fouling in sour heavy oil at elevated temperatures is an accumulation process in which both inorganic and carbonaceous matter deposit. Temperature significantly affects the build-up of deposits mainly by the formation of coke.
2. Generation of inorganic deposits such as iron sulphide is dominated by corrosion and increased with temperatures up to 390°C. At higher temperatures, the amount of inorganic species decreases somewhat, probably because the coke formed on the metal surface inhibits the corrosion reactions.
3. Surfaces tested can be divided into corroding and non-corroding alloys, depending on Cr content. Alloys between 15-20 % wt. Cr, serve as the boundary between low % Cr corroding surfaces, and high % Cr non-corroding surfaces.
4. CS and 9-chrome behave as corroding surfaces, yielding deposits high in ash at temperatures below 390°C. At temperature equal to or higher than 400°C, coking dominates and more than 80 % wt. of deposit is carbonaceous matters. Fe and S in deposits decline within small distances (~10μm) from the metal surface.
5. SS317, Incoloy 825 and Cr-CS behave as non-corroding surfaces, yielding deposits high in carbonaceous matter at all bulk temperature tested. Deposits on Cr-CS were 98%-99% carbonaceous matter. Incoloy 825 and SS317, with similar chromium content, yielded amounts and compositions of deposits close to those for the non-corroding materials. Fe and S in deposits remain constant at radial distances from the metal surface larger than 10μm.
6. Whether a deposit is solidly attached or loose depended on the proportion of ash it contained. Loose deposits occurred only when the ash content exceeded 70% wt.
7. Atomic ratios of Fe/S, Ni/Fe and V/Fe in oil, deposit and metals provide information on fouling mechanisms. For tested surfaces except Cr-CS, most of the Fe in the deposit is from corrosion of metal surfaces. For Cr-CS, Fe transfer is completely prevented by Cr layer, thus the trace of Fe in the deposit originates in the feed oil.

ACKNOWLEDGEMENT

The authors appreciate the support for this work by Syncrude Canada Ltd., and the technical input from Craig McKnight.

NOMENCLATURE

Cr-CS	chrome plated type 1018 low carbon steel
CS	type 1018 low carbon steel
d_{cyl}	diameter of cylinder, m
F	rotation speed of cylinder, rpm
MCR	micro carbon residue
r_{cyl}	radius of cylinder, m
Re	Reynolds number, dimensionless
SS317	type 317 stainless steel
u_{cyl}	rotation speed of cylinder, m/s
WD	working distance

GREEK

ω	rotation rate, rad/s
μ	dynamic viscosity of oil, Pa.s
ρ	density of oil, kg/m^3
τ_w	wall shear stress, Pa

REFERENCES

Albright, L. F. and Marek, J. C., 1988, Mechanistic model for formation of coke in pyrolysis units producing ethylene, *Industrial & Engineering Chemistry Research,* Vol. 27, pp. 755-759.

Delabrouille, F., Legras, L., Vaillant, F., Scott, P., B.Viguier and Andrieu, E., 2005, Effect of the Chromium Content and Strain on the Corrosion of Nickel Based Alloys in Primary Water of Pressurized Water Reactors, *Proc. 12th International Conference on Environmental Degradation of Materials in Nuclear Power System*, Salt Lake City, Utah, pp. 903-911.

Dickakian, G. and Seay, S., 1988, Asphaltene Precipitation Primary Crude Exchanger Fouling Mechanism, *Oil and Gas Journal,* Vol. 86, pp. 47-50.

Ebert, W. and Panchal, C. B., 1995, Analysis of Exxon crude-oil-slip stream coking data, *Proc. Fouling Mitigation of Industrial Heat-Exchangers Equipment*, San Luis Obispo, California, USA, pp. 451-460.

Efird, K. D., Wright, E. J., Boros, J. A. and Hailey, T. G., 1993, Correlation of Steel Corrosion in Pipe Flow with Jet Impingement and Rotating Cylinder Tests, *Corrosion,* Vol. 49, pp. 992-1003.

Gary, J. H. and Handwerk, G. E., 2001, *Petroleum Refining Technology and economics,* Marcel Dekker, Inc.

Lemke, H. K., 1999, Fouling in Refinery Equipment - An Overview, *Proc. AIChe National Spring Meeting*, pp. 375-382.

Lemke, H. K. and Stephenson, W. K., 1998, Deposit formation in industrial delayed coker/visbreaker heaters, *Petroleum Science and Technology,* Vol. 16, pp. 335-360.

Lugo, H. J. and Lunsford, J. H., 1985, The dehydrogenation of ethane over chromium catalysts, *Journal of Catalysis,* Vol. 91, pp. 155-166.

Mrowec, S., Walec, T. and Werber, T., 1969, High-temperature sulfur corrosion of iron-chromium alloys, *Oxidation of Metals,* Vol. 1, pp. 93-120.

Naka, M., Hashimoto, K. and Masumoto, T., 1979, Effect of addition of chromium and molybdenum on the corrosion behavior of amorphous Fe-20B, Co-20B and Ni-20B alloys, *Journal of Non-Crystalline Solids,* Vol. 34, pp. 257-266.

Pareek, V. K., Ramanarayanan, T. A., Mumford, J. D., Ozekcin, A. and Scanlon, J. C., 1994, The Role of Morphology and Structure in the Kinetic Evolution of Iron-Sulfide Films on Fe-Base Alloys, *Oxidation of Metals,* Vol. 41, pp. 323-341.

Parker, R. J. and McFarlane, R. A., 1999, Mitigation of Fouling in Bitumen Furnaces by Pigging, *Energy & Fuels,* Vol. 14, pp. 11-13.

Perry, R. H. and Green, D. W., 2007, *Perry's Chemical Engineers' Handbook,* McGraw-Hill Professional Publishing.

Reyniers, M.-F. S. G. and Froment, G. F., 1995, Influence of Metal Surface and Sulfur Addition on Coke Deposition in the Thermal Cracking of Hydrocarbons, *Industrial & Engineering Chemistry Research,* Vol. 34, pp. 773-785.

Romeo, G., Smeltzer, W. W. and Kirkaldy, J. S., 1971, Kinetics and Morphological Development of the Sulfide Scale on a Nickel‐20 w/o Chromium Alloy in Hydrogen Sulfide‐Hydrogen Atmospheres at 700°C, *J. Electrochem. Soc.,* Vol. 118, pp. 7.

Silverman, D. C., 1984, Rotating Cylinder Electrode for Velocity Sensitivity Testing, *Corrosion,* Vol. 40, pp. 220-226.

Taylor, W. F., 1976, Deposit Formation from Deoxygenated Hydrocarbons. II. Effect of Trace Sulfur Compounds, *Product R&D,* Vol. 15, pp. 64-68.

Turnbull, A., Slavcheva, E. and Shone, B., 1998, Factors Controlling Naphthenic Acid Corrosion, *Corrosion,* Vol. 54, pp. 922-930.

Wang, W. and Watkinson, A. P., 2011, Iron Sulphide and Coke Fouling from Sour Oils: Review and Initial Experiments, *Proc. International Conference on Heat Exchanger Fouling and Cleaning - 2011*, Crete Island, Greece, pp. 23-30.

Wiehe, I. A., 1993, A phase-separation kinetic model for coke formation, *Industrial & Engineering Chemistry Research,* Vol. 32, pp. 2447-2454.

Wiehe, I. A., 2008, *Process Chemistry of Petroleum Macromolecules,* CRC Press.

Zetlmeisl, M. J., 1996, Naphthenic Acid Corrosion and Its Control, *Proc. CORROSION 96*, Denver, Co.